Follicle-stimulating hormone increases bone mass in female mice

Charles M. Allan[1,2], Robert Kalak[1], Colin R. Dunstan, Kirsten J. McTavish, Hong Zhou, David J. Handelsman, and Markus J. Seibel

ANZAC Research Institute, University of Sydney, Concord Hospital, NSW 2139, Australia

Edited by John T. Potts, Massachusetts General Hospital, Charlestown, MA, and approved November 9, 2010 (received for review August 16, 2010)

Elevated follicle-stimulating hormone (FSH) activity is proposed to directly cause bone loss independent of estradiol deficiency in aging women. Using transgenic female mice expressing human FSH (TgFSH), we now reveal that TgFSH dose-dependently increased bone mass, markedly elevating tibial and vertebral trabecular bone volume. Furthermore, TgFSH stimulated a striking accrual of bone mass in hypogonadal mice lacking endogenous FSH and luteinizing hormone (LH) function, showing that FSH-induced bone mass occurred independently of background LH or estradiol levels. Higher TgFSH levels increased osteoblast surfaces in trabecular bone and stimulated de novo bone formation, filling marrow spaces with woven rather than lamellar bone, reflective of a strong anabolic stimulus. Trabecular bone volume correlated positively with ovarian-derived serum inhibin A or testosterone levels in TgFSH mice, and ovariectomy abolished TgFSH-induced bone formation, proving that FSH effects on bone require an ovary-dependent pathway. No detectable FSH receptor mRNA in mouse bone or cultured osteoblasts or osteoclasts indicated that FSH did not directly stimulate bone. Therefore, contrary to proposed FSH-induced bone loss, our findings demonstrate that FSH has dose-dependent anabolic effects on bone via an ovary-dependent mechanism, which is independent of LH activity, and does not involve direct FSH actions on bone cells.

animal model | gonadotropin | osteosclerosis | microcomputed tomography

Follicle-stimulating hormone (FSH) has a well-established role in reproduction. In females, FSH acts via the FSH receptor (FSHR) located in ovarian granulosa cells to control follicle development and steroidogenesis (1). Rising blood FSH levels are associated with female reproductive aging (2–4) because of diminished follicle-derived inhibin B (5–7), with elevated FSH generally preceding changes in serum luteinizing hormone (LH) or estradiol during perimenopause (3–5, 8). Sun et al. proposed that rising FSH levels with age may directly induce bone loss independent of estrogen deficiency (9). The authors reported that female mice deficient in FSH β-subunit ($Fshb^{-/-}$) or receptor ($Fshr^{-/-}$) were protected from bone loss despite estradiol deficiency, whereas haploinsufficient $Fshb^{+/-}$ females exhibited increased bone mass (9). By inference, it was proposed that elevated circulating FSH levels caused the bone loss observed in estrogen deficient peri- and postmenopausal women (9, 10). Mechanisms proposed for this putative FSH-induced bone loss included direct FSH stimulation of osteoclastic bone resorption via the FSHR (9) and FSH-induced TNFα production by bone marrow granulocytes and macrophages by as-yet-undefined pathways (11). However, elevated androgens in $Fshb^{-/-}$ and $Fshr^{-/-}$ female mice provide an alternate explanation for the preservation of bone mass in these estradiol-deficient mouse models (12). Although direct regulation of bone remodeling through FSH would have major clinical implications, such a mechanism has yet to exclude roles of FSH-regulated ovarian-derived factors, which, on a biological basis, are more likely to control bone turnover, such as sex steroids (12–15) or inhibins (16, 17).

In the current study, we have directly determined the effects of elevated FSH activity on bone mass and structure by using pituitary-independent, transgenic expression of human FSH (TgFSH) in female mice. Our TgFSH mouse model provides progressively rising circulating levels of FSH with age (18), with distinct transgenic lines allowing dose-dependent analysis of FSH actions in vivo (19–21). Using this FSH model, we have determined TgFSH actions on bone (*i*) in isolation of LH actions, using TgFSH expressed in hypogonadal (*hpg*) female mice lacking gonadotropin-releasing hormone (GnRH) and therefore endogenous FSH and LH secretion (21, 22), and (*ii*) in isolation of intact ovaries, using ovariectomized TgFSH mice (TgFSH-Ovx). In contrast to previous observations, our findings reveal that elevated FSH activity in vivo, regardless of LH and/or estradiol levels, markedly *stimulates* bone mass via an ovary-dependent pathway.

Results

TgFSH Stimulates Ovarian Secretion of Inhibin A and Testosterone As Well As Subnormal Estradiol Activity in *hpg* Mice. Serum levels of TgFSH driven by the rat insulin II gene promoter (21, 22) were significantly higher in $TgFSH^H$ compared with $TgFSH^m$ females (Fig. 1*A*). For each TgFSH mouse line (described in *Materials and Methods* and *SI Materials and Methods*), serum levels of TgFSH were equivalent on either the *hpg* or the non-*hpg* background (Fig. 1*A*). Circulating levels of inhibin A and testosterone were measured as indicators of TgFSH-stimulated ovarian function. Correspondingly, serum inhibin A levels were significantly higher in $TgFSH^m$ and $TgFSH^H$ (*hpg* and non-*hpg*) females relative to non-Tg controls (Fig. 1*C*). Serum testosterone levels were significantly higher in $TgFSH^H$ *hpg* females compared with $TgFSH^m$ *hpg* ($P < 0.01$) and non-Tg *hpg* ($P < 0.001$) females (Fig. 1*B*). Uterine weights were not changed in $TgFSH^m$ and $TgFSH^H$ non-*hpg* compared with WT (non-Tg, non-*hpg*) females, indicating no difference in biological estradiol activity (Fig. 1*D*). On the *hpg* background, uterine weights were increased in both $TgFSH^m$ *hpg* and $TgFSH^H$ *hpg* females compared with those in non-Tg *hpg* mice (Fig. 1*D*) but remained significantly lower than WT uterine weights, indicating subnormal estradiol activity in TgFSH-*hpg* females.

TgFSH Increases Bone Formation and Mass. Trabecular bone volume/tissue volume (BV/TV) was markedly increased in TgFSH compared with non-Tg female mice. Tibial BV/TV was significantly increased by ~2-fold and 5-fold ($P < 0.01$ and $P < 0.001$, respectively) in $TgFSH^m$ non-*hpg* and $TgFSH^m$ *hpg* females rel-

Author contributions: C.M.A., R.K., C.R.D., D.J.H., and M.J.S. designed research; C.M.A., R.K., K.J.M., and H.Z. performed research; C.M.A., R.K., C.R.D., H.Z., D.J.H., and M.J.S. analyzed data; and C.M.A., R.K., C.R.D., H.Z., D.J.H., and M.J.S. wrote the paper.

The authors declare no conflict of interest.

This article is a PNAS Direct Submission.

[1]C.M.A. and R.K. contributed equally to this work.

[2]To whom correspondence should be addressed. E-mail: charles@anzac.edu.au.

This article contains supporting information online at www.pnas.org/lookup/suppl/doi:10.1073/pnas.1012141108/-/DCSupplemental.

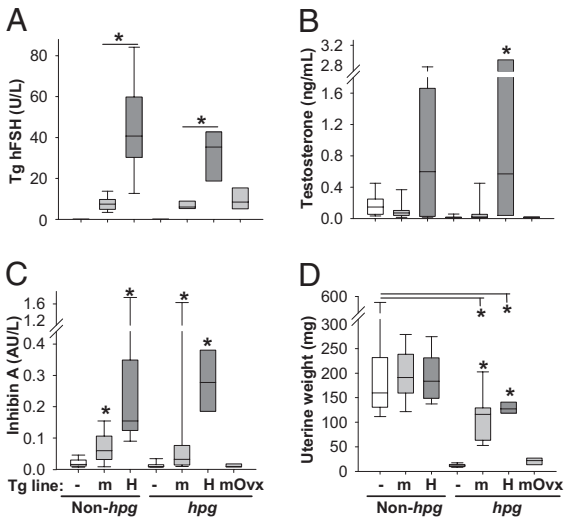

Fig. 1. TgFSH-induced changes to serum hormones and uterine weights. Groups comprised adult females from TgFSH^{m} (m) or TgFSH^{H} (H) lines and non-Tg (–) controls with non-*hpg* or *hpg* backgrounds (n = 7–26 mice per group). TgFSH^{m} *hpg* females were ovariectomized (Ovx) at 3 mo old (n = 7). Box plots show quartile values as box boundaries with median indicated by enclosed horizontal line and whiskers indicating 5th and 95th percentiles when definable (≥9 per group). As expected, serum TgFSH levels were up to 5-fold higher ($P < 0.01$) in TgFSH^{H} versus TgFSH^{m} females (*A*). TgFSH elevated ($P < 0.001$) serum testosterone (*B*) and inhibin A (*C*) in TgFSH^{H} *hpg* females compared with non-Tg controls. Compared with WT values, uterine weights from TgFSH^{m} or TgFSH^{H} non-*hpg* females were equivalent (*D*), whereas those from TgFSH^{m} *hpg* or TgFSH^{H} *hpg* females were lower ($P < 0.01$). Asterisk indicates significant differences ($P < 0.05$) between TgFSH and respective control groups or comparisons indicated by lines above.

ative to respective non-Tg controls (Fig. 2 *A* and *B* and Table S1). Compared with TgFSH^{m} mice, TgFSH^{H} females displayed higher bone mass with tibial BV/TV elevated up to 50-fold in TgFSH^{H} *hpg* ($P < 0.001$) and 11-fold in TgFSH^{H} non-*hpg* ($P < 0.001$) females versus non-Tg controls (Fig. 2 *A* and *B* and Table S1). Furthermore, vertebral trabecular BV/TV was significantly increased ∼4-fold and 5-fold ($P < 0.001$ for both) in TgFSH^{H} compared with non-Tg females on *hpg* or non-*hpg* genetic backgrounds, respectively (Fig. 2 *A* and *D* and Table S1). Very high FSH levels in TgFSH^{H} females stimulated de novo bone formation, filling marrow spaces with woven rather than lamellar bone, resembling bone formation induced by strong systemic anabolic stimuli. In TgFSH^{H} females, the process of woven bone formation appeared to be either continuing, with marrow spaces being actively filled as indicated by extensive calcein uptake (Fig. 2*G*), or approaching a maximal limit, with marrow spaces almost completely filled by bone with little detection of ongoing formation (Fig. 2*H*).

Mineral apposition rate and bone-formation rate per bone surface were all equivalent in the TgFSH^{m} versus non-Tg control females (Table S1). These rates could not be measured in TgFSH^{H} animals because of extensive woven bone formation in the metaphyseal region defined for dynamic histomorphometry, with extensive but blurred calcein uptake and lack of clear double labels (Fig. 2 *G* and *H*). Bone-formation rate per tissue volume increased by ∼6-fold ($P = 0.056$) in TgFSH^{m} non-*hpg* versus control females and was significantly elevated ∼2-fold ($P < 0.001$) in TgFSH^{m} *hpg* versus control *hpg* females (Table S1).

TgFSH Increases Bone Osteoblast but Not Osteoclast Surfaces. Examination of bone-forming osteoblast cells found that osteoblast surface relative to bone surface (Ob.S/BS) in tibia were increased in TgFSH^{H} non-*hpg* (+59%, $P < 0.001$) and TgFSH^{H} *hpg* (+49%, $P < 0.01$) females relative to the relevant control females but were similar to the relevant controls in TgFSH^{m} females on non-*hpg* or *hpg* backgrounds (Fig. 2*C* and Table S1). Consistent with these data were a positive correlation (exponential rise to maximal model) between increased Ob.S/BS and TgFSH levels on either the non-*hpg* ($r = 0.6$, $P < 0.001$) or *hpg* ($r = 0.5$, $P = 0.014$) background (i.e., combining data from both TgFSH lines). In contrast, analysis of bone-resorbing osteoclast cells found that osteoclast surface relative to bone surface (Oc.S/BS) was not significantly different between any experimental groups (Fig. 2*E* and Table S1). However, there was a negative correlation between Oc.S/BS and serum TgFSH on the non-*hpg* ($r = -0.3$, $P = 0.03$) background. In addition, there was a significant decline in osteoclast number per bone surface (N.Oc/BS) in TgFSH^{H} non-*hpg* (−45%, $P < 0.01$) and TgFSH^{m} *hpg* (−34%, $P < 0.05$) females, when compared with WT females (Table S1). Consistent with these data, there was a negative correlation ($r = -0.33$, $P = 0.013$) of N.Oc/BS with serum TgFSH levels in non-*hpg* mice.

Bone turnover markers suggested a complex or new steady state of bone remodeling may be present in mature TgFSH females. Circulating levels of N-terminal propeptide of type I procollagen (PINP), a marker of osteoblast activity, were similar in TgFSH versus non-Tg females on the non-*hpg* background, irrespective of the Tg line (Table S1). However, serum PINP levels were reduced in TgFSH^{m} *hpg* (−25%, $P < 0.05$) and TgFSH^{H} *hpg* (−34%, $P < 0.05$) compared with non-Tg *hpg* females (Table S1). In contrast, serum levels of tartrate-resistant acid phosphatase form 5b (TRACP5b), a bone-resorption marker, were significantly elevated (∼5-fold, $P < 0.001$) in TgFSH^{H} females on the non-*hpg* background and significantly higher in TgFSH^{m} *hpg* (+31%, $P < 0.01$) and TgFSH^{H} *hpg* (∼3-fold, $P < 0.01$) females compared with respective controls (Table S1).

TgFSH Effects on Bone Mass Requires and Is Correlated with Ovarian Function. Young mature TgFSH^{m} *hpg* females underwent ovariectomy to determine whether TgFSH effects on bone were independent of ovarian function. Loss of ovarian function in TgFSH^{m} *hpg*-Ovx females had no significant effect on serum levels of TgFSH (Fig. 1*A*), consistent with pituitary-independent Tg expression. In contrast, serum levels of inhibin A and testosterone both declined in TgFSH^{m} *hpg*-Ovx females to the levels observed in non-Tg *hpg* females (Fig. 1 *B* and *C*). Uterine weights in TgFSH^{m} *hpg*-Ovx mice strongly declined (−81%, $P = 0.001$), when compared with TgFSH^{m} *hpg* females, toward the values found in non-Tg *hpg* females (Fig. 1*D*). Ovariectomy completely removed the stimulatory effect of TgFSH on bone (Fig. 2 and Table S1). Tibial trabecular BV/TV was reduced in TgFSH^{m} *hpg*-Ovx females by 47% ($P < 0.01$) compared with non-Tg *hpg* mice (Fig. 2 *A* and *B* and Table S1). A similar ovariectomized-induced reduction was observed for vertebral trabecular bone (Fig. 2 *A* and *D* and Table S1). Loss of ovary function had distinct effects on circulating bone-formation or bone-resorption markers. Serum levels of TRACP5b (resorption) were lower (−17%, $P = 0.002$), whereas serum PINP (formation) levels were elevated (+54%, $P = 0.004$) in TgFSH^{m} *hpg*-Ovx compared with intact TgFSH^{m} *hpg* females (Table S1).

The ovary dependence of TgFSH effects was supported by correlation analysis performed separately for non-*hpg* and *hpg* mice to determine relationships between TgFSH and ovarian function markers (inhibin A and testosterone) with induced changes to tibial bone mass. By using the exponential rise to maximal (hyperbolic) model, there was a significant correlation between BV/TV and serum TgFSH (non-*hpg*: $r = 0.75$, $P < 0.0001$; *hpg* r: $= 0.78$, $P < 0.0001$), inhibin A (non-*hpg*: $r = 0.62$, $P < 0.0001$; *hpg*: $r = 0.76$, $P < 0.0001$), and testosterone (non-*hpg* background: $r = 0.33$, $P < 0.005$; *hpg* females: $r = 0.89$, $P < 0.001$) consistent with a dose-dependent ceiling effect of FSH on bone mass (Fig. 3

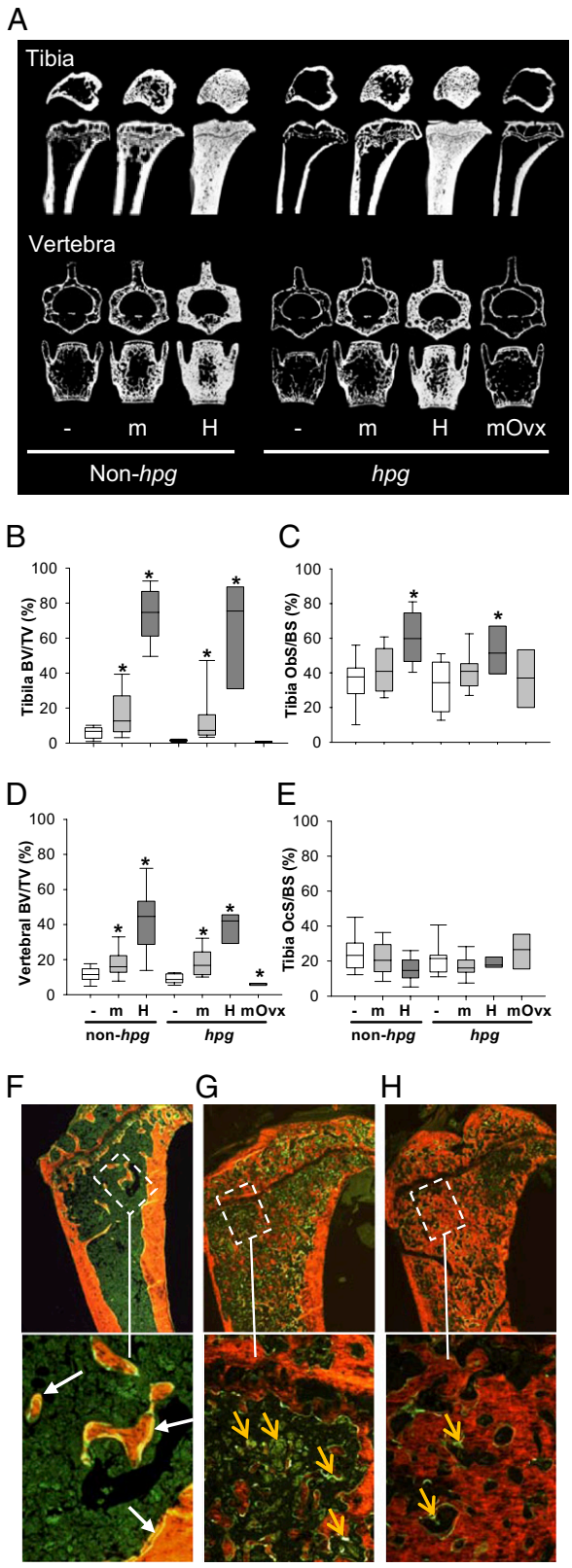

Fig. 2. TgFSH increased bone mass in adult female mice. (*A*) Representative longitudinal and cross-sections of proximal tibia taken 0.5 mm below growth plate and middle of L3 vertebra (μCT) are shown. Histomorphometry used bones from all collected TgFSH^{m} (n = 26 non-*hpg* or 16 *hpg*), TgFSH^{H} (n = 15 non-*hpg* or 8 *hpg*), TgFSH^{m} *hpg*-Ovx (n = 7), and non-Tg (n = 19 non-*hpg* or 18 *hpg*) females. (*B–E*) Box plots show quartile values as box boundaries with median indicated by enclosed horizontal line and whiskers indicating 5th and 95th percentiles when definable (≥9 per group). TgFSH increased trabecular BV/TV (μCT) in tibia ($P < 0.01$) of TgFSH females (*B*) and vertebra ($P < 0.001$) of TgFSH^{H} females (*D*, non-*hpg* or *hpg*) versus respective non-Tg controls. Asterisk indicates significant differences ($P < 0.05$) between TgFSH and respective control groups. Tibial trabecular Ob.S/BS or Oc.S/BS (static histomorphometry) show a trend for increased Ob.S/BS and normal Oc.S/BS in TgFSH versus non-Tg females (*C* and *E*). (*F–H*) Calcein (green) and xylenol orange staining show normal bone in WT with expected calcein double labels (*F*, white arrows) compared with bone in TgFSH^{H} females exhibiting marrow spaces actively being filled with woven bone as indicated by extensive diffuse calcein uptake (*G*, orange arrows) or almost completely filled by woven bone with little ongoing formation as indicated by reduced calcein uptake (*H*, orange arrows). (Magnification: *Upper*, 40×; *Lower*, 200×.)

A–C). Optimal model fits were for individual curves for non-*hpg* and *hpg* mice for inhibin A and testosterone, whereas for TgFSH a single global model for both groups combined was the best fit.

Absence of FSHR mRNA Expression in Bone and Bone-Derived Cells. To determine whether TgFSH may interact with known FSHRs in bone, we examined *Fshr* mRNA expression in bone by RT-PCR. Despite clear detection of expected *Fshr* mRNA in ovary, there was no detectable *Fshr* expression in bone or cultured osteoblast or osteoclast RNA preparations (Fig. 3*D*). Furthermore, analysis of *Fshr* expression during osteoclast formation (days 0, 3, and 7) from either spleen or macrophage-like RAW 264.7 cells failed to detect any predicted PCR product (Fig. S1), even after a secondary round of PCR (40 cycles) using primary PCR samples as template. Osteocalcin (OCN) or calcitonin receptor (CTR) mRNA expression by RT-PCR provided distinct markers for osteoblasts or osteoclasts, respectively (Fig. 3*D*).

Discussion

Transgenic expression of FSH in female mice stimulated an unexpected and striking increase in both appendicular and axial bone mass. This significant and reproducible effect was independent of LH activity and occurred in the presence of reduced biological estrogen action. Our findings show that the skeletal response to FSH requires the presence of functional ovaries, consistent with the role of FSH in ovarian function. The current results further imply that circulating FSH has no direct stimulatory effect on bone in vivo.

Bone histomorphometry revealed that TgFSH dose-dependently increased the trabecular bone volume fractions in tibia and vertebra of female mice. Mice with the lower range of circulating TgFSH (TgFSH^{m} line) had significantly increased bone mass and were previously shown to exhibit normal serum LH and estradiol levels (18), suggesting the FSH effect on bone was independent of ovarian estradiol secretion. Higher levels of circulating FSH (TgFSH^{H} line) induced more pronounced bone-mass accrual with distinct patterns of de novo bone formation, suggesting the presence of a strong anabolic stimulus. We predict that FSH-induced osteosclerosis is caused by an increased bone-formation rate, consistent with the strong trend for increased bone formation at the tissue level, and significantly increased Ob.S/BS in TgFSH^{H} females. Positive and negative correlations observed between TgFSH and Ob.S/BS and N.Oc/BS, respectively, in non-*hpg* females are consistent with the marked increase in bone mass. Serum levels of bone markers PINP and TRACP5 (as single endpoint measurements) did not relate to the increased bone mass in aged TgFSH mice; however, sustained high FSH levels may induce a new steady state in bone density, with the bone-formation rate per bone surface showing adaptation to the high FSH effects with a higher bone density set point. This finding is consistent with longitudinal studies of PINP levels in rats treated with anabolic doses of parathyroid hormone, in which PINP was elevated after 3 wk but similar to baseline levels after 7 wk of

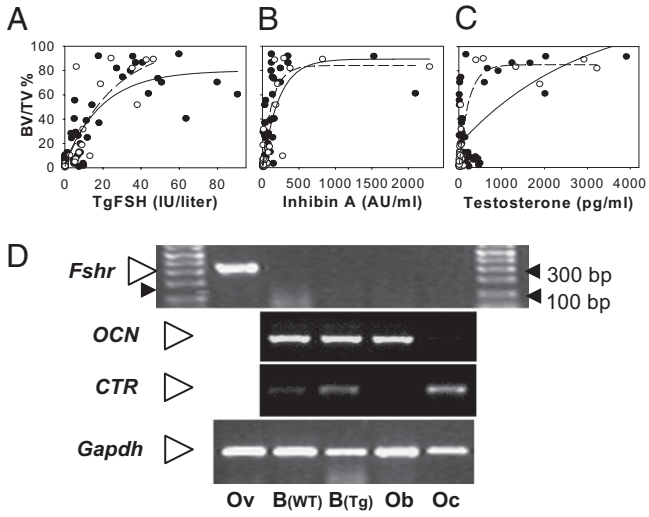

Fig. 3. Increased bone mass correlated with serum hormone levels in TgFSH females. (*A–C*) Scatter plots and correlation lines (Sigmaplot version 10 Wizard Correlation) for tibial trabecular BV/TV (%) versus serum TgFSH (*A*) or ovarian-derived serum inhibin A (*B*) or testosterone levels (*C*) shown as solid lines and filled circles for non-*hpg* data or dashed lines and open circles for *hpg* data. Data were combined for $TgFSH^m$ and $TgFSH^H$ lines on either the non-*hpg* (FSH, $n = 54$; inhibin A, $n = 42$; testosterone, $n = 57$) or *hpg* (FSH, $n = 32$; inhibin A, $n = 34$; testosterone, $n = 41$) background. Correlations indicated an exponential rise to maximal BV/TV associated with increasing levels of all serum hormones measured. (*D*) Mouse *Fshr* mRNA expression was detected (RT-PCR) in adult ovary (Ov) as expected but not in long bone from either $TgFSH^H$ (Tg) or non-Tg (WT) adult females or in isolated cultured mouse osteoblast (Ob) or osteoclast (Oc) preparations. CTR or OCN mRNA expression confirmed differentiated Oc or Ob cells, respectively. *Gapdh* mRNA was used as internal cDNA control, and *Fshr* findings repeated in triplicate.

treatment (23), indicating that PINP levels fall when a new high–bone mass steady state is established, even with ongoing anabolic treatments.

FSH-induced bone formation in GnRH-deficient *hpg* females demonstrated that the mechanisms responsible for bone-mass accrual are independent of GnRH and LH activity. Moreover, uterine weights in all TgFSH *hpg* females remained subnormal compared with WT mice, indicative of subphysiological estradiol effects. Elevated FSH levels in conjunction with the decreased estradiol state in these TgFSH-*hpg* females resemble the progressive changes to circulating FSH/estradiol levels in peri- and postmenopausal women (3, 24). Thus, the increased bone mass observed in TgFSH-*hpg* females appears inconsistent with the recent proposal that high FSH causes estradiol-independent bone *loss* in perimenopausal women exhibiting rising FSH and declining estradiol levels (10). Furthermore, severe bone loss in FSH-deficient (nontransgenic) *hpg* compared with WT female mice demonstrates that FSH is not required for driving low bone mass in aging females.

Bone formation in TgFSH females depended on ovarian function. Removal of intact ovaries abolished the increase in bone mass found in TgFSH *hpg* females, with bone values in TgFSH-Ovx females reduced to levels similar to those observed in hormone-deficient non-Tg *hpg* females. An ovarian-dependent pathway for FSH-induced bone formation was further supported by positive correlations observed between circulating ovarian-derived factors, such as inhibin A and testosterone, and increased bone mass in the TgFSH females. The strong correlation between increasing serum inhibin A levels and elevated bone mass may indicate involvement of the inhibin/activin pathway or functional association with FSH-induced follicular development. Although there is evidence that inhibins may directly suppress osteoblastogenesis and osteoclastogenesis (25), transgenic expression of human inhibin A in mice showed that continual exposure has an anabolic effect on bone mass (26). The current findings are consistent with a regulatory role for inhibin A in bone mass, although increased bone mass was found in $TgFSH^m$ females exhibiting levels of inhibin A well within the normal range. Likewise, the correlation between serum testosterone levels in TgFSH females exhibiting increased bone mass implicates a role for steroid-induced bone formation, presumably via local aromatization of androgen to estradiol and direct estradiol receptor mechanisms in the bone (27). The present study cannot distinguish between the effects of specific ovarian factors in vivo, such as sex steroids or inhibins. However, the absolute requirement of ovarian function for FSH-induced bone mass is consistent with recent studies in $Fshr^{-/-}$ mice that suggested a critical role for ovarian secretory products in maintaining bone mass and not the absence of FSH action (15). Combined, these findings demonstrate that mouse models investigating mechanisms of FSH-induced changes to bone dynamics must reconcile associated changes to ovarian-derived products, including inhibins and sex steroids. Consistent with our findings showing that FSH effects on bone require ovarian function, a recent study of postmenopausal women demonstrated that suppression of FSH to premenopausal levels (in the presence of hormonally nonresponsive ovaries) had no effect on bone-resorption markers (28).

The present study found no detectable expression of mouse *Fshr* mRNA in bone or cultured osteoblasts preparations, noting that *Fshr* mRNA was readily detected in ovary samples. Likewise, we did not detect *Fshr* mRNA in cultured osteoclast preparations (derived from spleen or macrophage-like RAW 264.7 cells), by using highly sensitive RT-PCR analysis, despite recent evidence for low-level *FSHR* mRNA expression in mouse (9) or human (29) osteoclasts. The present study used primers to amplify a 3′ region (spanning exons 7–10) present in all reported spliced variants of mouse *Fshr* found in the ovary (30) and would be capable of detecting both the normal and variant (lacking exon 9) *FSHR* reported to be expressed in human monocyte and osteoclast preparations (29). Levels of *FSHR* expression in human osteoclasts were acknowledged to be extremely low (29), yet our present study failed to detect any bone or osteoclast expression of mouse *Fshr* even after an additional round of PCR amplification. No details were previously provided to compare primer sets and PCR conditions that detect *Fshr* expression in mouse bone and osteoclasts (9). Our present findings reveal that known mouse *Fshr* isoforms are not expressed in bone or osteoclasts. Considered together with the requirement of a functional ovary for TgFSH-induced bone formation, we propose that FSH stimulatory actions do not involve direct FSH interaction in bone.

We conclude that elevated FSH causes bone formation and increased bone mass in female mice. This FSH-induced effect required ovarian function but was independent of GnRH or LH activity. These effects were consistent with the positive association of FSH-induced ovarian secretion of inhibin or testosterone with elevated bone mass, whereas we find no evidence for direct FSH stimulatory actions in the bone.

Materials and Methods

Transgenic FSH Mice and Experimental Groups. The two independent transgenic lines expressing TgFSH were (*i*) the αβ.6 line expressing serum TgFSH levels up to ~10 IU/L (18), here designated $TgFSH^m$ to denote a *m*oderate elevation of FSH activity, and (*ii*) the 113 line, with higher serum TgFSH levels up to ~41 IU/L (21), here designated $TgFSH^H$ for *h*igher FSH activity. TgFSH *hpg* females were obtained by crossbreeding $Gnrh1^{+/-}$ animals and genotyped by detection of WT ($Gnrh1^{+/+}$ *or* $Grnh1^{+/-}$, each considered non-*hpg*), *hpg* ($Grnh1^{-/-}$), and TgFSH PCR products as described (21, 31). Animals were housed at the ANZAC Research Institute using procedures approved by the Sydney South West Area Health Services' Animal Welfare Committee

and consistent with the National Health and Medical Research Council code of practice for animal experimentation. Mature $TgFSH^m$ and $TgFSH^H$ females having either non-*hpg* or *hpg* backgrounds and non-*hpg* or *hpg* littermate/age-matched non-Tg female controls were collected between 6 and 19 mo of age to increase exposure to higher TgFSH levels in older mice (described in *SI Materials and Methods*). Anesthetized $TgFSH^m$ *hpg* females were ovariectomized at 3 mo of age then collected at 8 mo of age to examine the requirement of intact ovaries for FSH actions on bone. Experimental groups are summarized in Table S1.

Blood and Tissue Collection and Preparation. For dynamic histomorphometry, mice received calcein (10 μg/g body weight i.p.) at 10 and 3 d before being euthanized. Blood was collected from anesthetized females, then the uteruses were dissected and weighed. In each mouse, both tibiae and the lumbar vertebra (L2, L3, and L4) were dissected, fixed, and processed for static histomorphometry or μCT analysis (*SI Materials and Methods*), and a humerus was dissected for RNA isolation. Vertebrae were kept in PBS until μCT. One tibia was decalcified, paraffin-embedded, and serially sectioned for static histomorphometry. The contralateral tibia was stored in 70% ethanol, then embedded, and sections were cut and stained in xylenol orange for μCT analysis (*SI Materials and Methods*).

Histomorphometry. Histomorphometric analysis of the proximal tibial metaphysis was conducted in all mice. Measurements of static indices were performed on longitudinal sections stained with tartrate-resistant acid phosphate (TRAP) to identify osteoclasts and stained with hematoxylin/eosin or Safranin-O for general histology (*SI Materials and Methods*). N.Oc/BS and Oc.S/BS were measured. Osteoblasts were identified by morphology to calculate Ob.S/BS. Calcein fluorescence (green) indicated active mineralization, visualized against xylenol orange fluorescence in bone. In the area of the metaphyseal bone defined for dynamic histomorphometry, single and double calcein labels provided bone-surface lengths for unlabeled bone, single- and double-labeled bone, and the interlabel width, from which the mineral apposition rate and bone-formation rate were calculated (*SI Materials and Methods*).

Microcomputed Tomography. Tibiae and lumbar vertebrae (L3) were analyzed by μCT using a Skyscan 1172 scanner (*SI Materials and Methods*). Defined regions in transverse sections of tibial cortical or tibial trabecular bone, and the entire volume of trabecular bone within the vertebral body were selected for morphometric analysis of bone indices (*SI Materials and Methods*). Trabecular morphology was described by measuring BV/TV, trabecular number (Tb.N.), trabecular separation (Tb.Sp.), trabecular thickness (Tb.Th.), and bone surface to bone volume ratio (32).

Serum Hormones and Bone Markers. Serum levels of TgFSH were determined by a species-specific immunoassay as described (21, 33). Serum inhibin A levels were determined by a human inhibin A ELISA modified for assaying mouse serum as described in ref. 34 and *SI Materials and Methods*. Serum testosterone levels were quantified using liquid chromatography/tandem mass spectrometry (LC-MS/MS) as described (35). Uterus weight was used as an established biological indicator of estradiol actions in vivo because of the lack of a reliable method to measure serum estradiol levels in female mice (35, 36). Serum levels of PINP and TRACP5b, markers of osteoblast or osteoclast activity, respectively, were measured by immunoassay (*SI Materials and Methods*).

Expression of Mouse FSHR mRNA. Total RNA was prepared from ovary, long bone, and cultured osteoblastic cells prepared from calvaria of neonatal C57BL/6J mice (37) as well as osteoclast cultures prepared from (*i*) spleen cells from adult C57BL/6J mice (38) and (*ii*) the murine RAW 264.7 cell line (*SI Materials and Methods*). Mouse *Fshr* mRNA expression was detected by RT-PCR using SuperScript III (Invitrogen) for first-strand cDNA synthesis and conditions (55 °C annealing, primers 5′-ACACAACTgTgCATTCAACgg-3′ and 5′-gACTTgTTgCAAATTggATgA-3′) to amplify a 329-bp product spanning exons 7–10, present in all *Fshr* mRNA variants found in mouse ovary (30). CTR and OCN mRNA expression was detected by RT-PCR using primer pairs 5′-CCACTgAgCCTTCATTTCCT-3′/5′-TgCCTgCTTTCCTACgAAC-3′ and 5′-CCTTCATgTCCAAgCAggA-3′/5′-TgCCTgCTTTCCTACgAAC-3′, respectively. Mouse *Gapdh* was detected for sample cDNA normalization.

Statistical Analysis. Data are presented as medians with interquartile range unless otherwise stated. Kruskal–Wallis test was performed to determine significant differences between experimental groups. Mann–Whitney *U* test was used for selected pairwise comparisons only if Kruskal–Wallis test showed significant difference between groups. Nonlinear regression was performed using routines implementing automatic generation of initial values and the Marquardt algorithm for minimizing squared deviations from suitable preset models (exponential rise to maximum in Sigmaplot or hyperbola in Prism). Data for non-*hpg* and *hpg* mice were compared by determining Akaike information criterion for the global (shared parameters) model with that for individual curve fits. Statistical analysis was performed using SPSS 16 (SPSS Inc.), Sigmaplot version 10 (Systat Software), and Prism version 5 (GraphPad Software).

ACKNOWLEDGMENTS. We thank Tim Harwood, Mark Jimenez, Julian Kelly, Janine Street, Li Laine Ooi, and staff at the Nanostructural Analysis Network Organisation (NANO) Major National Research Facility/Electron Microscope Unit, University of Sydney, for technical support. We thank Mark Hedger and Susan Haywood for the inhibin A assay (Monash Institute of Medical Research, Monash University, Victoria, Australia). This work was supported by National Health and Medical Research Council Australia Grant 512545.

1. Simoni M, Gromoll J, Nieschlag E (1997) The follicle-stimulating hormone receptor: Biochemistry, molecular biology, physiology, and pathophysiology. *Endocr Rev* 18: 739–773.
2. Lenton EA, Sexton L, Lee S, Cooke ID (1988) Progressive changes in LH and FSH and LH: FSH ratio in women throughout reproductive life. *Maturitas* 10:35–43.
3. Robertson DM, Hale GE, Fraser IS, Hughes CL, Burger HG (2008) A proposed classification system for menstrual cycles in the menopause transition based on changes in serum hormone profiles. *Menopause* 15:1139–1144.
4. Sherman BM, Korenman SG (1975) Hormonal characteristics of the human menstrual cycle throughout reproductive life. *J Clin Invest* 55:699–706.
5. Klein NA, et al. (1996) Decreased inhibin B secretion is associated with the monotropic FSH rise in older, ovulatory women: A study of serum and follicular fluid levels of dimeric inhibin A and B in spontaneous menstrual cycles. *J Clin Endocrinol Metab* 81: 2742–2745.
6. Reame NE, Wyman TL, Phillips DJ, de Kretser DM, Padmanabhan V (1998) Net increase in stimulatory input resulting from a decrease in inhibin B and an increase in activin A may contribute in part to the rise in follicular phase follicle-stimulating hormone of aging cycling women. *J Clin Endocrinol Metab* 83:3302–3307.
7. Robertson DM, et al. (2009) Interrelationships between ovarian and pituitary hormones in ovulatory menstrual cycles across reproductive age. *J Clin Endocrinol Metab* 94:138–144.
8. Lee SJ, Lenton EA, Sexton L, Cooke ID (1988) The effect of age on the cyclical patterns of plasma LH, FSH, oestradiol and progesterone in women with regular menstrual cycles. *Hum Reprod* 3:851–855.
9. Sun L, et al. (2006) FSH directly regulates bone mass. *Cell* 125:247–260.
10. Zaidi M, et al. (2007) Proresorptive actions of FSH and bone loss. *Ann N Y Acad Sci* 1116:376–382.
11. Iqbal J, Sun L, Kumar TR, Blair HC, Zaidi M (2006) Follicle-stimulating hormone stimulates TNF production from immune cells to enhance osteoblast and osteoclast formation. *Proc Natl Acad Sci USA* 103:14925–14930.
12. Seibel MJ, Dunstan CR, Zhou H, Allan CM, Handelsman DJ (2006) Sex steroids, not FSH, influence bone mass. *Cell*, 127:1079, author reply 1080–1081.
13. Baron R (2006) FSH versus estrogen: Who's guilty of breaking bones? *Cell Metab* 3: 302–305.
14. Prior JC (2007) FSH and bone—Important physiology or not? *Trends Mol Med* 13:1–3.
15. Gao J, et al. (2007) Altered ovarian function affects skeletal homeostasis independent of the action of follicle-stimulating hormone. *Endocrinology* 148:2613–2621.
16. Martin TJ, Gaddy D (2006) Bone loss goes beyond estrogen. *Nat Med* 12:612–613.
17. Gaddy D (2008) Inhibin and the regulation of bone mass. *Curr Osteoporos Rep* 6: 51–56.
18. McTavish KJ, et al. (2007) Rising follicle-stimulating hormone levels with age accelerate female reproductive failure. *Endocrinology* 148:4432–4439.
19. Allan CM, et al. (2004) Complete Sertoli cell proliferation induced by follicle-stimulating hormone (FSH) independently of luteinizing hormone activity: Evidence from genetic models of isolated FSH action. *Endocrinology* 145:1587–1593.
20. Allan CM, Handelsman DJ (2005) Transgenic models for exploring gonadotropin biology in the male. *Endocrine* 26:235–239.
21. Allan CM, et al. (2001) A novel transgenic model to characterize the specific effects of follicle-stimulating hormone on gonadal physiology in the absence of luteinizing hormone actions. *Endocrinology* 142:2213–2220.
22. Allan CM, et al. (2006) Follicle-stimulating hormone increases primordial follicle reserve in mature female hypogonadal mice. *J Endocrinol* 188:549–557.
23. Komatsu DE, et al. (2009) Longitudinal in vivo analysis of the region-specific efficacy of parathyroid hormone in a rat cortical defect model. *Endocrinology* 150:1570–1579.

24. Rannevik G, et al. (2008) A longitudinal study of the perimenopausal transition: Altered profiles of steroid and pituitary hormones, SHBG and bone mineral density. *Maturitas* 61:67–77.
25. Gaddy-Kurten D, Coker JK, Abe E, Jilka RL, Manolagas SC (2002) Inhibin suppresses and activin stimulates osteoblastogenesis and osteoclastogenesis in murine bone marrow cultures. *Endocrinology* 143:74–83.
26. Perrien DS, et al. (2007) Inhibin A is an endocrine stimulator of bone mass and strength. *Endocrinology* 148:1654–1665.
27. Vico L, Vanacker JM (2010) Sex hormones and their receptors in bone homeostasis: Insights from genetically modified mouse models. *Osteoporos Int* 21:365–372.
28. Drake MT, McCready LK, Hoey KA, Atkinson EJ, Khosla S (2010) Effects of suppression of follicle-stimulating hormone secretion on bone resorption markers in postmenopausal women. *J Clin Endocrinol Metab* 95:5063–5068.
29. Robinson LJ, et al. (2010) FSH-receptor isoforms and FSH-dependent gene transcription in human monocytes and osteoclasts. *Biochem Biophys Res Commun* 394:12–17.
30. O'Shaughnessy PJ, McLelland D, McBride MW (1997) Regulation of luteinizing hormone-receptor and follicle-stimulating hormone-receptor messenger ribonucleic acid levels during development in the neonatal mouse ovary. *Biol Reprod* 57:602–608.
31. Singh J, O'Neill C, Handelsman DJ (1995) Induction of spermatogenesis by androgens in gonadotropin-deficient (hpg) mice. *Endocrinology* 136:5311–5321.
32. Hahn M, Vogel M, Pompesius-Kempa M, Delling G (1992) Trabecular bone pattern factor—A new parameter for simple quantification of bone microarchitecture. *Bone* 13:327–330.
33. Jimenez M, et al. (2005) Validation of an ultrasensitive and specific immunofluorometric assay for mouse follicle-stimulating hormone. *Biol Reprod* 72:78–85.
34. Wang Y, et al. (2005) Gonadotropin control of inhibin secretion and the relationship to follicle type and number in the hpg mouse. *Biol Reprod* 73:610–618.
35. Harwood DT, Handelsman DJ (2009) Development and validation of a sensitive liquid chromatography-tandem mass spectrometry assay to simultaneously measure androgens and estrogens in serum without derivatization. *Clin Chim Acta* 409: 78–84.
36. McNamara KM, et al. (2010) Measurement of sex steroids in murine blood and reproductive tissues by liquid chromatography-tandem mass spectrometry. *J Steroid Biochem Mol Biol* 121:611–618.
37. Zhou H, Mak W, Zheng Y, Dunstan CR, Seibel MJ (2008) Osteoblasts directly control lineage commitment of mesenchymal progenitor cells through Wnt signaling. *J Biol Chem* 283:1936–1945.
38. Zhou H, et al. (2001) A novel osteoblast-derived C-type lectin that inhibits osteoclast formation. *J Biol Chem* 276:14916–14923.